

Optical and Thermal Performance Analysis of a Steady Spherical Collector with a Crescent-shaped Rotating Absorber

Thierry S. M. Ky¹, Boureima Dianda¹, Moktar Ousmane^{1,2}, Magloire Pakouzou¹, Sié Kam¹, Dieudonné J. Bathiebo¹

¹Laboratory of Renewable Thermal Energies, UFR-SEA, 03 BP 7021, University Ouaga I Pr Joseph KI-ZERBO, Burkina Faso.

²University of Agadez PO BOX 199 Niger.

Abstract— In this paper, optical analysis of spherical concentrator is made to determine the local and the global geometric concentration, as knowing the geometric concentration of a system can help predict what temperatures can possibly be obtained with it. This leads to conclude that spherical collectors may produce higher temperatures than parabolic trough, and they could even be sharply improved by using a mixt cylindrical and cavity (or flat) absorber.

A craft prototype of a steady spherical concentrator made with concrete and having a smooth inner surface mapped with mirror tape is presented. Its absorber is made with blacken steel sheets and shaped like a moon crescent to be aligned with the declination plan and to avoid motorization for the tracking of the sun from East to West. Experimental measurements lead to temperatures reaching 686°C on the curve of the least diffusion, and 252°C in the absorber oven-like reservoir. Overall, the results suggests higher potentialities of spherical collectors, which also show possibility of use with much reduced tracking system and less vulnerability to bad weather.

Keywords—Fixed Mirror Distributed Focus-FMDF, Mixt conical and cavity absorber. Optical analysis, Spherical collector, Solar Bowl.

I. INTRODUCTION

Cooking bread requires temperatures between 250°C and 300°C. To do so with solar systems, we need a concentrator that tracks the sun. Scheffler systems (Muniret *al.*, 2010[1]) are designed for developing countries as less heavy in care, and use hot air for cooking bread. Even so, Scheffler systems installed in Burkina Faso-West Africa had shown poor resistance to bad weather and a quite dependency to the daily presence of a mechanic to adjust the plant concentrators for tracking the declination.

A recent study made by Mahdi and Bellel 2014 [2] tends to suggest that hemispherical concentrator has interesting mean concentration ratio, because it is used for focusing in one spot. This also had been studied by Kyet *al.*, 2015 [3] who proposed the use of hemispherical concentrator to replace Scheffler systems. The geometric mean concentration of the hemispherical concentrator had been restudied to best locate the plan of the least diffusion and to determine the size of the cavity absorber to be disposed. For a record, the geometric mean concentration is advocated when the target is a flat or cavity absorber.

In this paper, we study the geometric concentration of a hemispherical concentrator and determine the size of the absorber to dispose along the axis of reflection. Knowing the geometric concentration of a system can help predict what can possibly be obtained as temperatures. Then, a prototype using crescent-shaped absorber is studied. That absorber is placed in the plan of declination so that it can be easily rotated for adjustment, and works without any motorized system for tracking the sun from East to West.

II. GEOMETRIC CONCENTRATION OF A HEMISPHERICAL CONCENTRATOR

The hemispherical concentrator does not focus on one point. It focuses on the axis parallel to the solar rays and passing through the center of the sphere. It is on this axis that an absorber (or receiver) needs to be placed (Fig.1). A study shows that the reflection position on the axis is obtained by the following formula (El-Refaie, 1987 [4], Ng *et al.*, 2012 [5], Bouguetaia, 2013 [6]),

$$Y(\phi, n) = \sqrt{1 - R^2} + (-1)^n \frac{\sin \phi}{\sin(2n\phi)} - R \cot(2n\phi) \quad (1)$$

With the ratio R equal the radius of the cylindrical axis of the absorber R_{aa} on the radius of the hemispherer r_s ,

The optical image is proportional to the radius of the absorber since the optical spot covers the absorber. Fig.2 shows a relationship between R_{aa} and y .

$\frac{R_{aa}}{r_s} = (1 - y) \sin \theta_s$ for $y = \frac{Y}{r_s}$. So $Y(\phi, n)$ can be defined using equations (5) and (6),

$$Y(\phi, n) = r_s \left[1 + (-1)^n \frac{\sin \phi}{\sin(2n\phi)} \right] \tag{7}$$

2.3. Definition of the geometric concentration $C_{g(Cir_3D)}$:

We will define a local geometric concentration (or local geometric concentration ratio) $C_{g(Cir_3D)}$ as the variation of concentration along the absorber for any half angle ϕ ; it is the concentration of a partial area projected to the corresponding partial area of the absorber. This will allow to determine the way temperature are distributed along the conical absorber.

We will also define a global geometric concentration $C_{g(Cir_3D)}$ as the concentration of an entire area of the concentrator to its entire corresponding absorber for an aperture half angle ϕ_s .

In the following optical study, we will consider the frontal area of the spherical concentrator always facing the sun and all the rays projected on the conical absorber. The landmark will be with the origin at the junction between the absorber and the concentrator and the y axis going toward the center of the sphere.

The local geometric concentration along the absorber $C_{g(Cir_3D)}$ is the interpolation of the ratios of the elementary surface of reflection from the hemispheric concentrator on the elementary surface of projection on the absorber. These surfaces may be defined as follows (Fig. 3):

* The elementary surface reflected by the concentrator,

$$S_{sph}(\phi_{i+1} - \phi_i) = \pi r_s^2 \left[\sin^2(\phi_{i+1}) - \sin^2(\phi_i) \right] \tag{8}$$

* The elementary surface of projection on the absorber using equations (5) and (7),

$$S_{rec}(\phi_{i+1} - \phi_i, n) = 2\pi \frac{R_{aa}(\phi_{i+1}, n) + R_{aa}(\phi_i, n)}{2} \left[Y(\phi_{i+1}, n) - Y(\phi_i, n) \right] \tag{9}$$

* The elementary (or local) geometric concentration is obtained using equations (8) and (9) as,

$$c_g(\phi_{i+1} - \phi_i, n) = \frac{S_{sph}(\phi_{i+1} - \phi_i)}{S_{rec}(\phi_{i+1} - \phi_i, n)}$$

and:

$$c_{g(Cir_3D)}(\phi_{i+1} - \phi_i, n) = \frac{1}{\sin \theta_s} \frac{\sin^2(\phi_{i+1}) - \sin^2(\phi_i)}{|A^2(\phi_{i+1}, n) - A^2(\phi_i, n)|}$$

with: $A(\phi, n) = \frac{\sin \phi}{\sin(2n\phi)}$ (10)

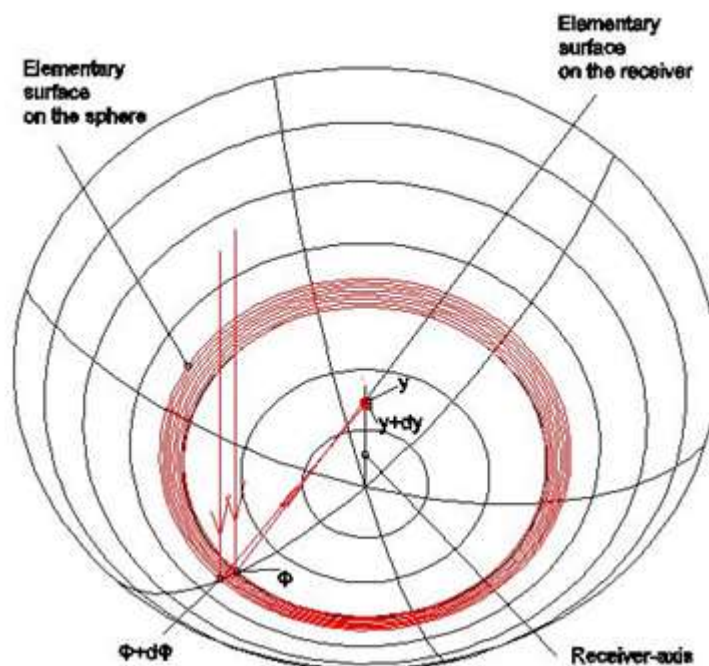


Fig. 3: Elementary surfaces for geometric concentration calculation

$C_{g(Cir_3D)}(\phi_{i+1} - \phi_i, n)$ is an algorithm that determines the geometric concentration in any location of the absorber (ie the local geometric concentration) as well as the global geometric concentration. The parameter i varies in the range $\phi \in [\theta_s; 90^\circ]$ depending on the chosen step of discretization (Fig.3).

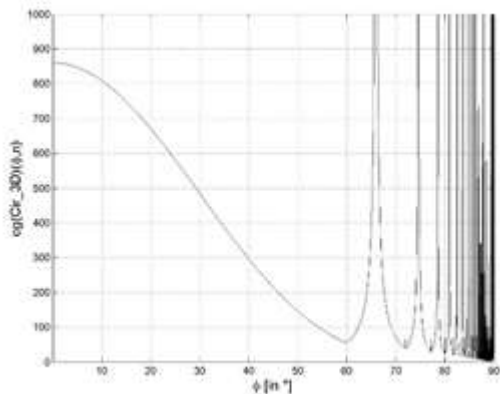
We used MATLAB program to define a new function based on y (with $y = \frac{Y}{r_s}$ and $0 \leq y \leq 0,5 - \sin \theta_s$) rather than ϕ ,

so the curve of the local geometric concentration along the absorber can be drawn (Fig.4).

The curves show a maximum of 860 reached for $\phi = \sin \theta_s$ (or $y \approx 0,5 - \sin \theta_s$) that progressively decrease to 76 (for $\phi = \sin \theta_s$ or $y \approx 0,08$). Then we notice multiple reflections.

Observations:

* Multiple reflections generate concentration peaks in the



vicinity of the lower end of the conical absorber, thereby creating a zone of heat very close to the surface of the concentrator.

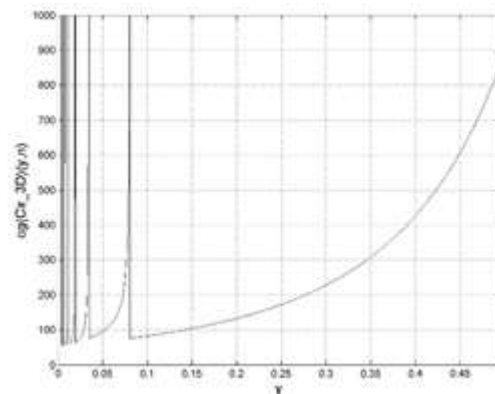


Fig.4: Curves of local geometric concentration along the absorber depending on Φ or y

* The second curve of Fig.4 is fairly concise in comparison with the optical concentration ratio values measured on a similar system in Texas (Stine *et al.*, 1986 [8]) (Fig.5). The curve of the Texas system, however, shows a rise of concentration near the contact zone between the concentrator and absorber. This is due to the superposition (overlapping) phenomenon of optical images of the sun generated by multiple reflections.

$$c_{g(Cir_3D)}(y) = \sum_{j=1}^{2n-1} c_{g(Cir_3D)}(y, n(j))$$

(11)

That gives the following curve using MATLAB program (Fig. 6).

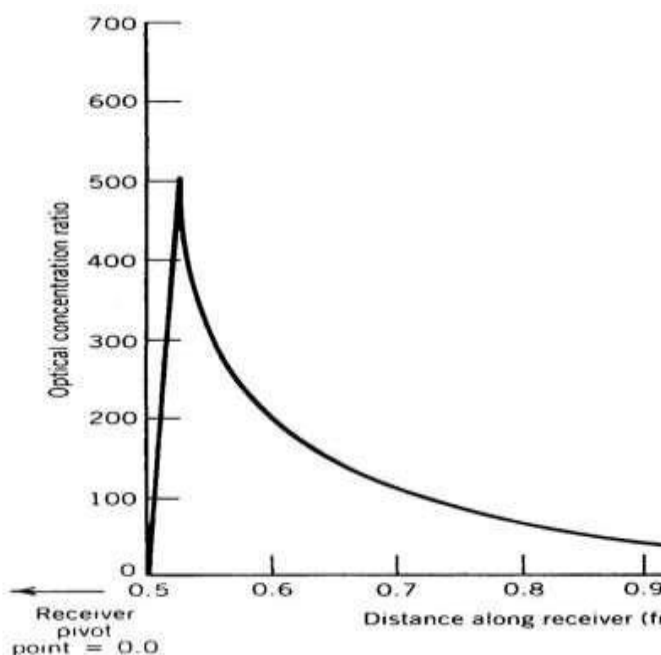


Fig.5: Flux distribution along the absorber of a FMDF collector. (Stine *et al.*, 1986)

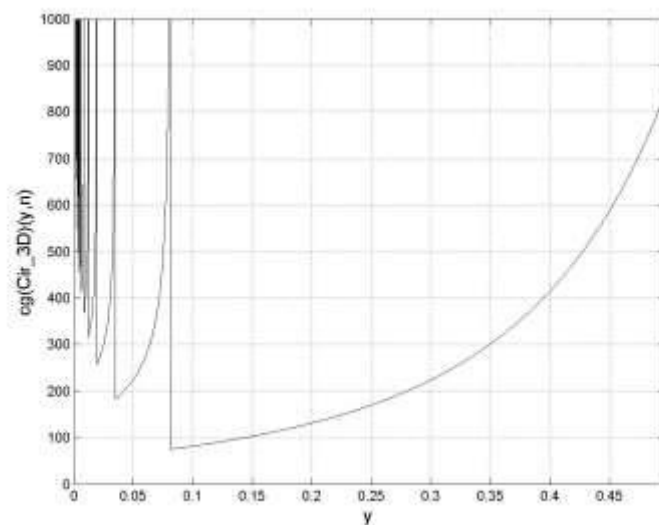


Fig.6: Local geometric concentration considering the superposition phenomenon

Taking into account the superposition phenomenon will bring us to sum all local geometric concentrations depending on the number of reflections. Equation to use is,

Studying the local geometric concentration allows to understand the way the absorber is used. Usually, the fluid flows from bottom to top, because it flows from the part with low local concentration (meanwhile lesser heat) to the part with higher concentration (higher heat). The FMDF absorber is also shaped as a cone and water inlet is from the lower part (Fig. 7).

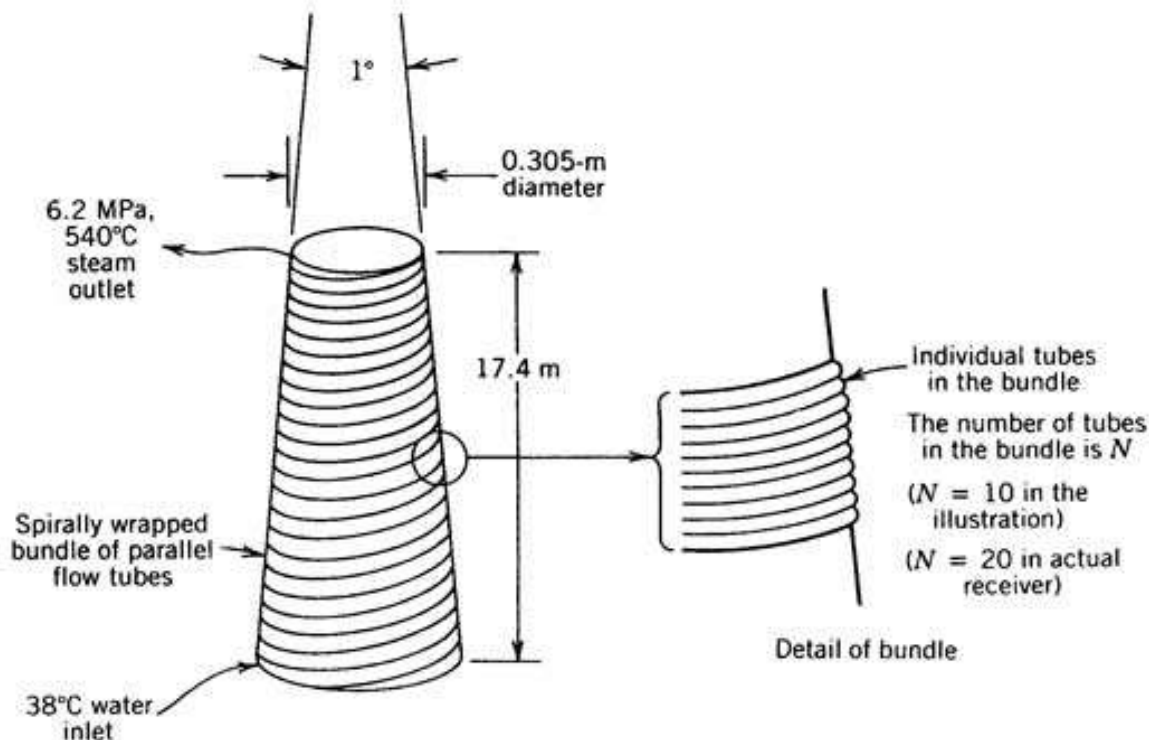


Fig.7: Schematic diagram of the absorber for FMDF collector. Courtesy of Santia National Laboratories. Built at Crosbyton-Texas-USA.

2.4. Linearization of the function $c_{g(Cir_3D)}(\phi_{i+1} - \phi_i, n)$

:
 Since all geometric concentrations are determined directly as a function of ϕ parameter, the function $c_{g(Cir_3D)}(\phi_{i+1} - \phi_i, n)$ can also be expressed likewise. This linearization is obtained for $n = 1$, ie by excluding the multiple reflections and focusing exclusively on the interval $\phi_s \in [0; 60^\circ]$ (or on the interval

$y \in [0; 0,5 - \sin \theta_s]$). We obtain the following functions as linearization of equation (10) with their plots (Fig.8),

$$c_{g(Cir_3D)}(\phi) = \frac{4}{\sin \theta_s} \cos^4 \phi \tag{12}$$

$$\text{and } c_{g(Cir_3D)}(y) = \frac{1}{4(y-1)^4 \sin \theta_s} \tag{13}$$

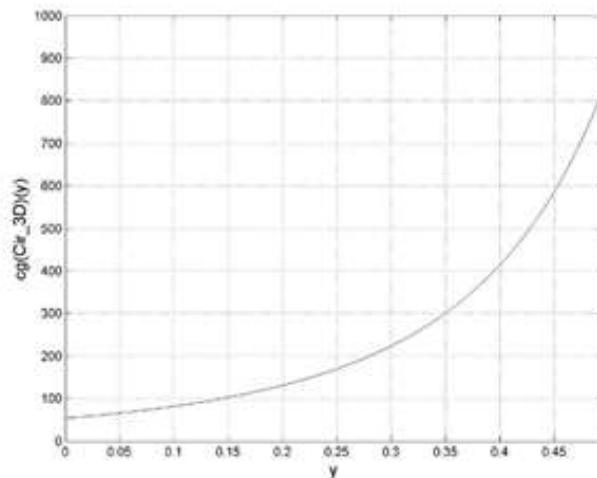
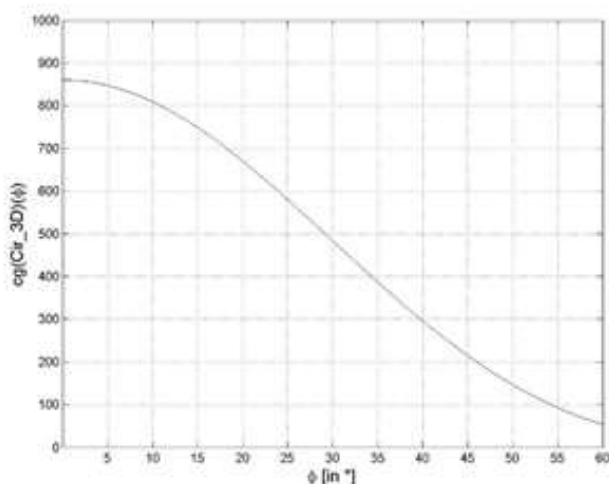


Fig. 8: Linearization of local geometric concentration depending on Φ and y

2.5. Validation domain for $C_{g(Cir_3D)}$:

This equation is meaningless for small values of ϕ . Indeed, the sunspot covers almost the entire surface of the absorber for these small values. However, it is very precise for the side rays. Moreover, the equation considers the homogeneous sunspot in one hand, and the juxtaposition effect of the sun rays rather than the superposition effect on the other hand. (Veynant, 2011) [9].

2.6. The global geometric concentration $C_{g(Cir_3D)}$.

The global geometric concentration (which is usually called geometric concentration) $C_{g(Cir_3D)}$ is determined by using the equation (10) and by fixing ϕ_i to 0° and ϕ_{i+1} to ϕ_s . The equation therefore becomes,

$$C_{g(Cir_3D)}(\phi_s) = \frac{4}{\sin \theta_s} \cos^2 \phi_s \text{ for } \phi_s \leq 60^\circ \quad (14)$$

This equation concretely shows the increase of the size of the conical absorber with the half angle ϕ_s till it reaches its limits to $h = \frac{r_s}{2}$ when $\phi_s = 60^\circ$ (Fig.9). Then, since the size of the absorber will not increase any longer while the projected area of the concentrator is still increasing and projecting towards the conical absorber, the equation (14) of the global concentration shifts to,

$$C_{g(Cir_3D)}(\phi_s) = \frac{4}{3 \sin \theta_s} \sin^2 \phi_s \text{ for } \phi_s > 60^\circ \quad (15)$$

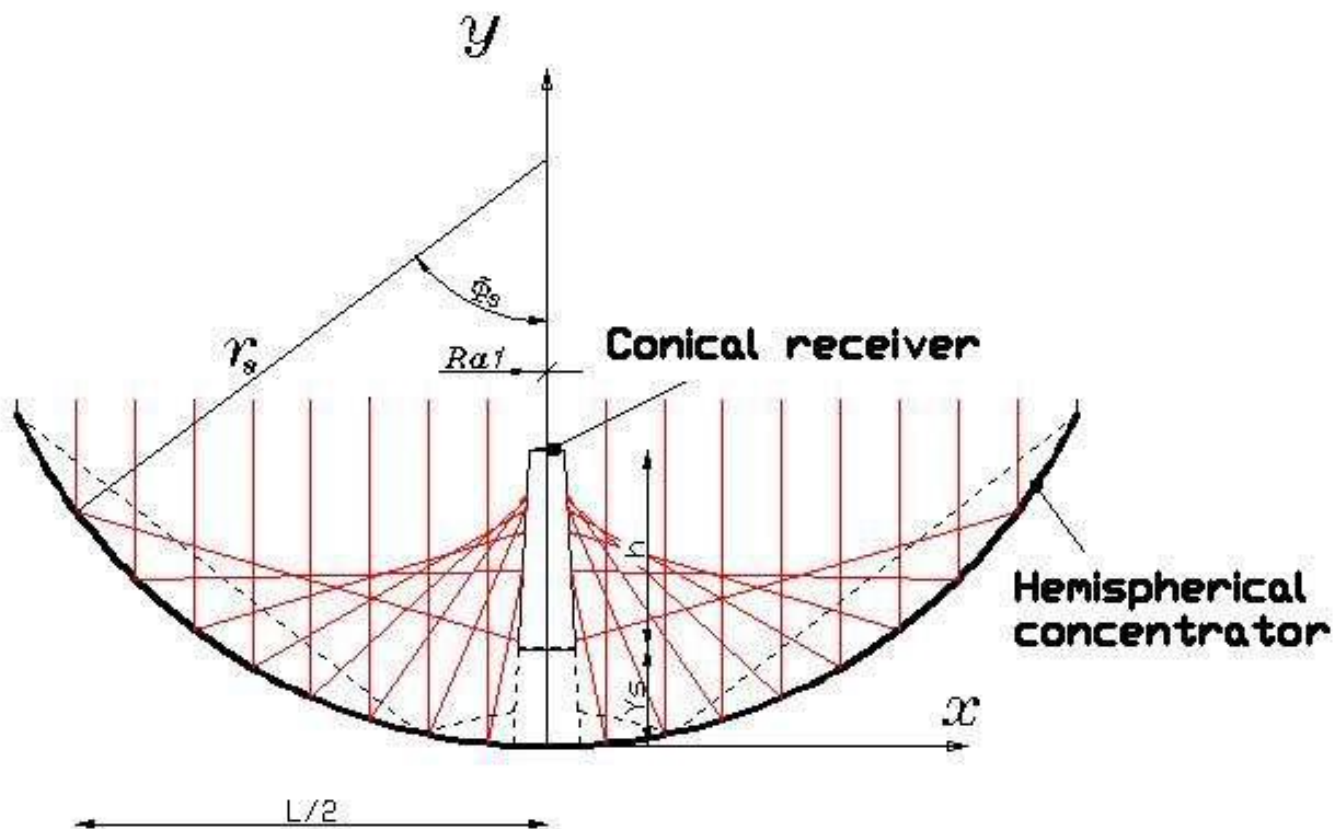


Fig.9: Concentrator projecting to its conical absorber. The wider the circle' radius ($L/2$), the higher the cone until $\phi_s = 60^\circ$ when h is maximum. Afterwards, multiple projections continue to reach the conical absorber.

The plot of equations (14) and (15) is given on the following fig. 10

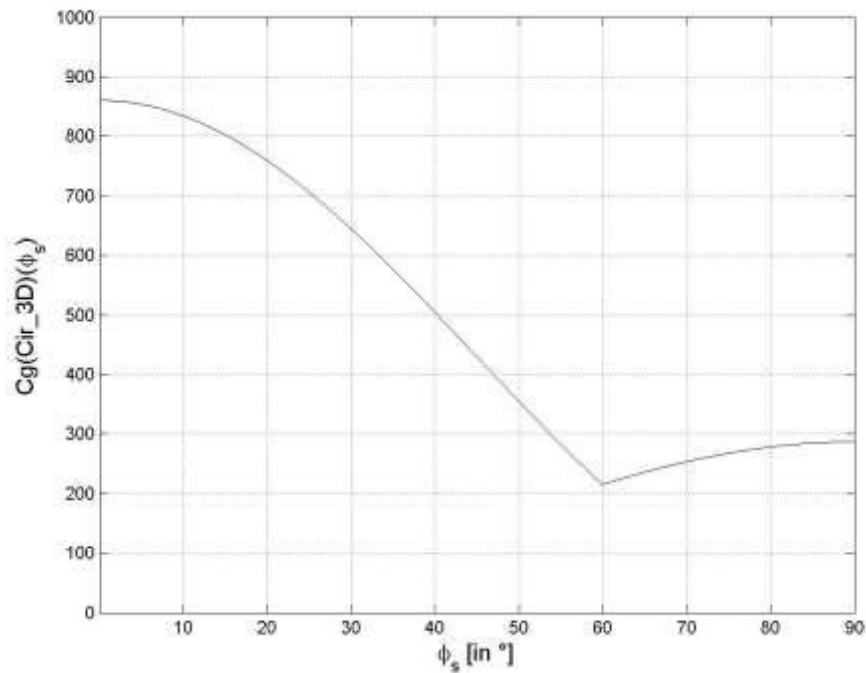


Fig. 10: Global geometric concentration depending on ϕ_s . With the increase of the size of the absorber, the geometric concentration sharply decreases from 860 to 215. Then since the absorber size no longer evolves, the geometric concentration increases to 287.

The global concentration can also be defined to express the change of the height h of the conical absorber by the equation:

$$C_{g(\text{Cir}_{3D})}(y) = \frac{1}{(1-y_s)^2 \sin \theta_s} \quad (16)$$

so setting $y_s = \frac{1}{2} - \frac{h}{r_s}$ leads to $C_{g(\text{Cir}_{3D})}\left(\frac{h}{r_s}\right) = \frac{1}{\left(\frac{1}{2} + \frac{h}{r_s}\right)^2 \sin \theta_s}$ with $\frac{h}{r_s} \in \left[\sin \theta_s; \frac{1}{2}\right]$ (17)

The plot of equation(17) is given on the following fig. 11:

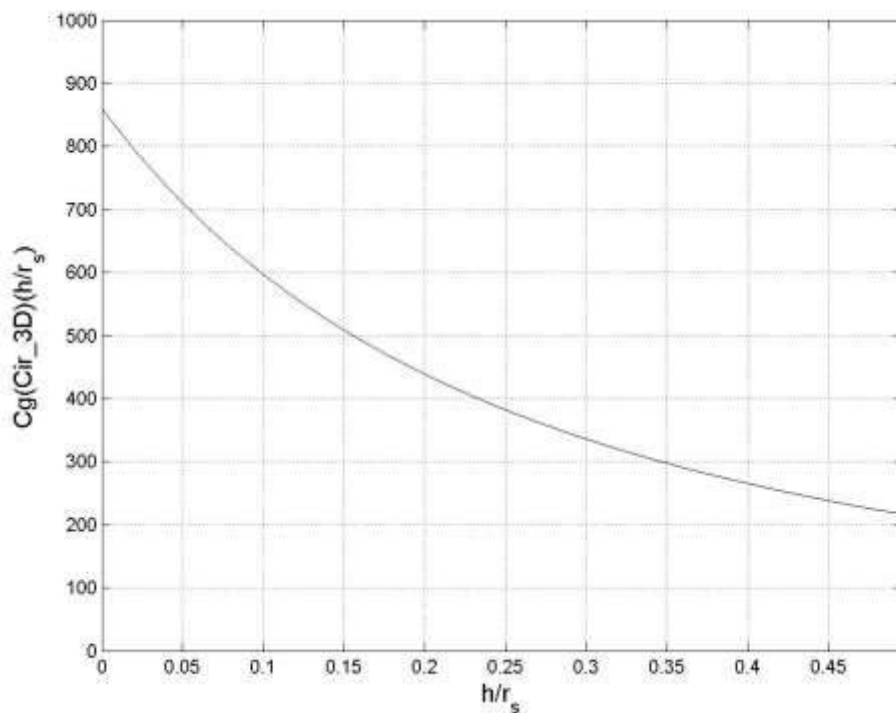


Fig. 11: Global geometric concentration depending on $\frac{h}{r_s}$. The conical absorber starts from $\frac{h}{r_s} = \sin \theta_s$. This is where the cone begins to grow while the geometric concentration is at its maximum (860). Then, the conical absorber has its full height at $\frac{h}{r_s} = 0,5$, and the geometric concentration had decreased from 860 to 215.

Multiple reflections are not taken into account in the equation (17) and fig. 11.

2.7. Real global geometric concentration of the system:

If the concentrator system studied above is designed using flat mirrors tiles of 5 cm x 5 cm for example, it is possible to introduce Δl , characterizing the linear dispersion caused by such tiles. Using equations (16) and (17), we obtain,

$$C_{g(Cir_3D)}(\phi_s) = \frac{4}{\Delta l + \sin \theta_s} \cos^2 \phi_s \text{ for } \phi_s \leq 60^\circ \quad (18)$$

$$\text{and } C_{g(Cir_3D)}(\phi_s) = \frac{4}{3(\Delta l + \sin \theta_s)} \sin^2 \phi_s \text{ for}$$

$$\phi_s > 60^\circ \quad (19)$$

Note: A dispersion is generally represented by a half-angle $\Delta \theta$. In this case, $(\Delta l + \sin \theta_s)$ should be replaced by $\sin(\Delta \theta + \theta_s)$ in the preceding equations (18) and (19).

2.8. Comparisons between hemispheric global geometric concentration $C_{g(Cir_3D)}$ and geometric mean concentration $C_{gmed(Cir_3D)}$.

From the previous results on the geometric concentration reachable for a parabolic trough (215), we can consider that using a hemispherical concentrator already guarantees a higher temperature in comparison with the parabolic trough. But when we also use the result of geometric mean concentration of a hemispherical concentrator known from previous publications (Kyet *et al.*, 2015, Bernard *et al.*, 1980[10]), we notice that for the values of angle ϕ_s below 23° (angle taken from the center of the sphere), a cavity (or flat) absorber is more suggested to be used, for the curve of geometric mean concentration is above that of the geometric concentration as we can see on fig. 12. This geometric mean concentration reaches a maximum at $\phi_s = 11^\circ$ to a value of 2.964. Actually, the hemispheric concentrator is one of the concentrators with a geometric mean concentration

higher than its geometric concentration. Beyond 23°, a use of conical absorber is compulsory.

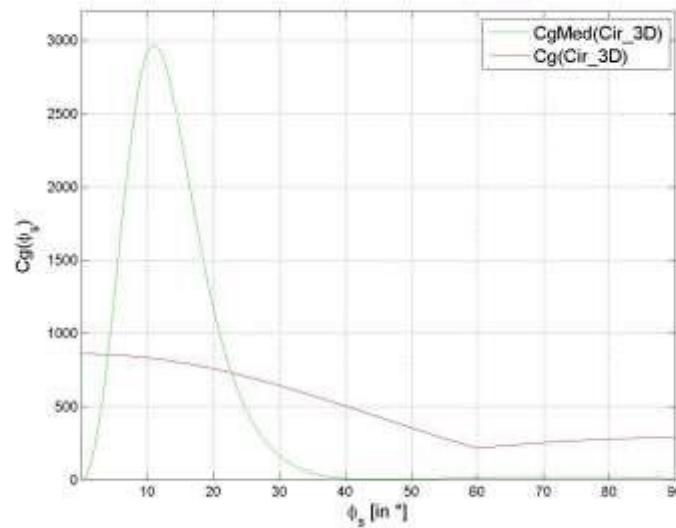


Fig. 12: curves comparing global geometric concentration and geometric mean concentration of a hemispherical concentrator. We see that $C_{gmed(Cir_3D)} \geq C_{g(Cir_3D)}$ for angle $\phi_s \leq 23^\circ$ suggesting the use of a cavity absorber in that zone. When beyond that value, it would be compulsory to use a conical absorber.

It is quite common to see a mixt use of cavity and conical absorber on the same hemispherical concentration system. That will be a good solution to optimize the system by having the fluid admitted from the lower inlet of a conical receiver to the upper outlet in a cavity absorber. The cavity absorber will best contribute if the area projecting into it has a half angle $\phi_{s1} < 23^\circ$ as shown in fig. 13. As a matter of fact, Sulaiman *et al.*, 1997 [11] used this particularity of FMDF collector to suggest a hybrid photovoltaic and thermal receiver to dispose.

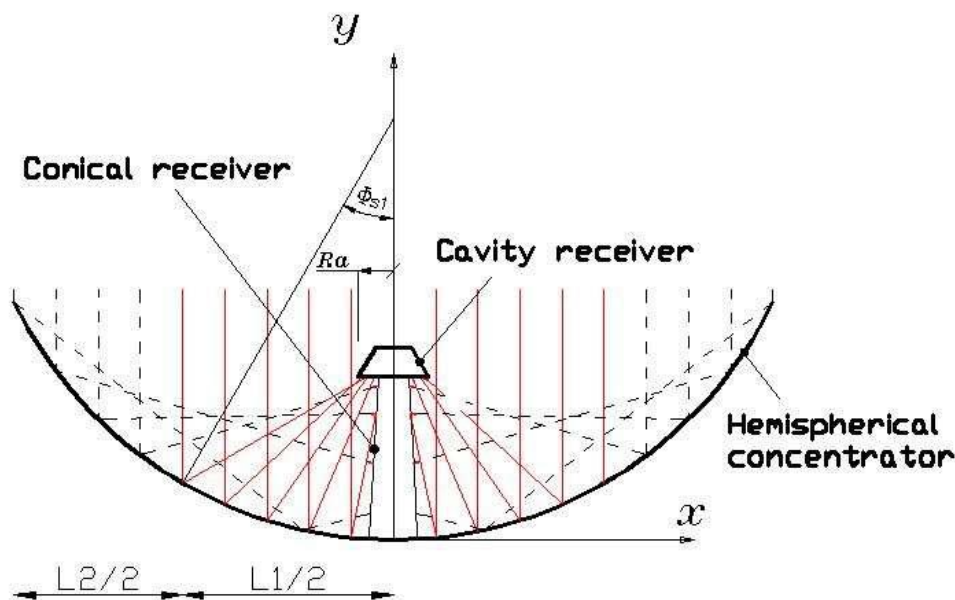


Fig.13: Hemispherical concentrator with a mixt conical and cavity absorber

III. THERMAL PERFORMANCE ANALYSIS ON A PROTOTYPE

The spherical concentrator was conceived with concrete to get a smooth inner surface. A taping film of mirror was used to get the reflective surface. The circular frontal area has a diameter of 1,14m. The sphere inner diameter is 1,18m (Fig. 14).



Fig.14: Image of the prototype - Concrete hemispherical concentrator with it moon crescent-like absorber.

The absorber is made of steel sheet painted in black. It has a closing reservoir, and we are concerned in having the air temperature inside the reservoir. The absorber has a lip at its bottom that is designed to be in the curve of the least diffusion, meanwhile, the bottom part of the reservoir receives sunlight as a plate corresponding to a geometric mean concentration with a half angle of 22°C (Fig.15).

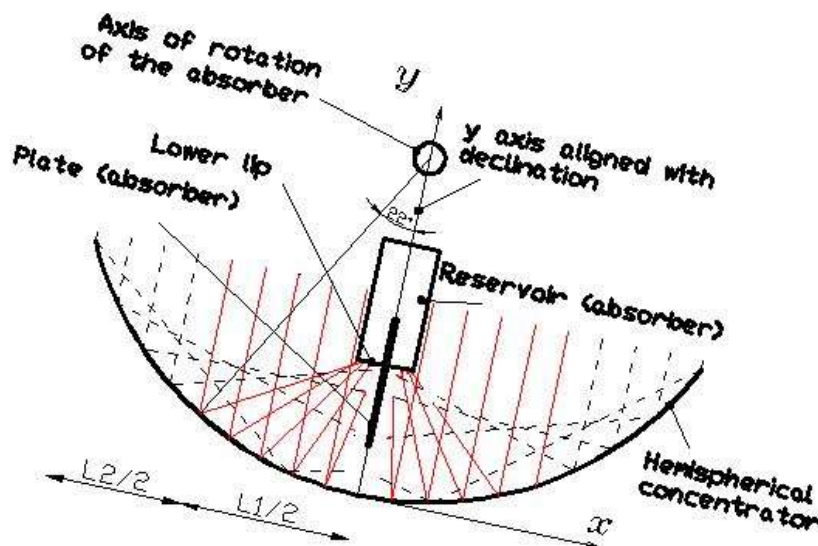


Fig.15: Schematic design of the prototype with its reservoir and plate absorber aligned in the declination plan.

There is also a plate in the middle that receives sunlight in the place of a conical absorber. After all, the absorber was design shaped like a moon crescent to be positioned in the plan of declination such that there will be no need to track the sun from East to West, and the tracking for the

declination is obtained by a rotation of the absorber along an axis passing through the center of the sphere.

3.1. Materials and methods.

Following materials and methods were used to get our results:

- A data logger type Midi LOGGER GL200A of GRAPHTEC brand.
- Probes A and B are placed against bottom lip of the receiver in both sides (North and South) to measure the temperature in the focal point. To do this, we follow the light spot indicating the reflection of the sun to search for the highest temperature. We follow the sun's path every 5 minutes.
- Probes C and D are placed inside the reservoir in both side East and West 10 cm from the closet. They will get the inner air temperature, so they are not in contact with any surface.

- Probe Amb. reports the ambient temperature.
- A type SL100 and brand KIMO solarimeter is used to measure solar radiation.

3.2. Results and discussions about the measurements of June 06, 2016:

The curves A and B (Fig. 16) grow progressively till 11.a.m. when they reach a pic of 686°C. This follows at some point the irradiation curve of the day which had an average of 750 W.m⁻² (Fig. 17). The curves of probes A and B not being continuous indicates the difficulty to get the focal points.

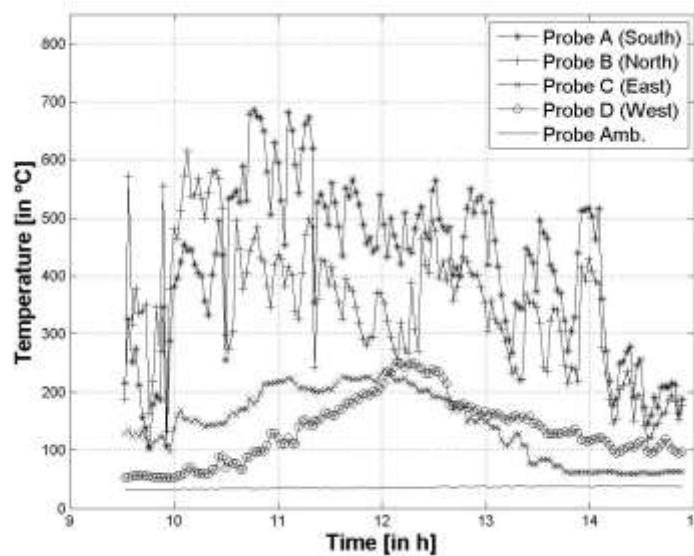


Fig.16: temperature curves on June 06, 2016.

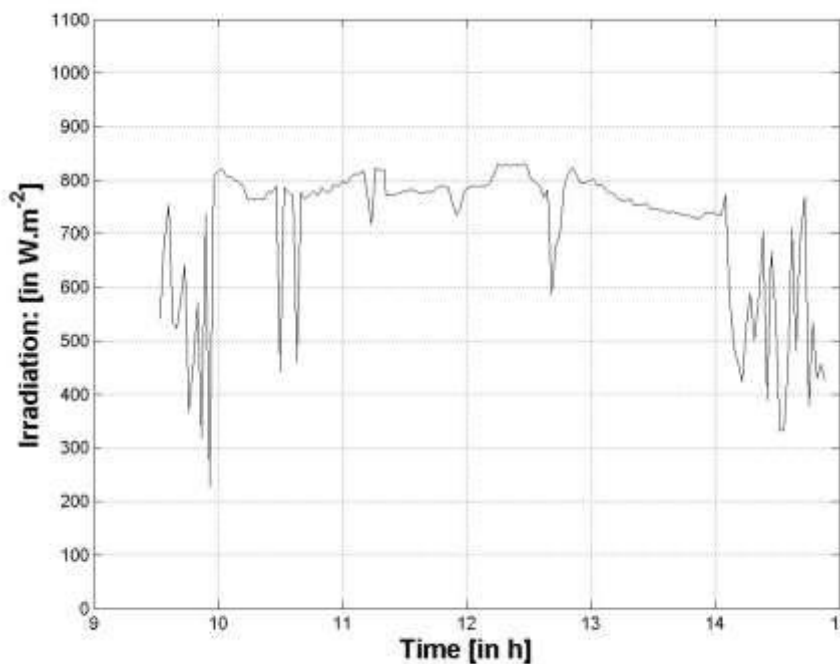


Fig.17: Irradiation curve on June 06, 2016.

Temperatures above 500°C are already reached around 9.30.a.m. and are also kept till 2.10.p.m, which allow us to state that if the absorber was perfectly aligned with the declination plan, temperatures well above 500°C will be maintained from 9.30 a.m. to 2.10 p.m.

Temperatures inside the absorber, considering maximum reached by probes C and D, are ranged between 97°C and 252°C. To some points, these temperatures could have been improved if the reservoir's North and South sides were better prepared to limit heat losses.

IV. CONCLUSION

We have made an optical analysis of a hemispherical concentrator, showing how the local concentration evolves along an axis absorber which is conical. A global geometric concentration curve had been also drawn for comparison with geometric mean concentration.

From this analysis, we notice that the geometric concentration of a hemispherical concentrator is always higher than that of a parabolic trough, telling us that the hemispheric system gives higher temperature than parabolic trough. Moreover, the hemispherical concentrator could do better if it is used with mixed conical and cavity (or plate) absorber with respect to the projection angles of the sunlightsizing the cavity.

From the prototype, high temperatures could be obtained with a hemispherical concentrator: 686°C maximum at the focal lip, and 252°C maximum for the air inside the absorber reservoir. This is still less than what was obtained by the Crosbyton courtesy in Texas-USA (540°C of steam generated by an only conical absorber), but suggests higher potentialities of hemispherical concentrators, which additionally show possibility of use with much reduced tracking system and less vulnerability to bad weather.

REFERENCES

- [1] Munir, A., Hensel, O. and Scheffler, W., 2010. Design principle and calculations of a Scheffler fixed focus concentrator for medium temperature applications. *Solar Energy* 84: 1490-1502.
- [2] Mahdi, K., Bellel, N., Development of a spherical solar collector with a cylindrical receiver. *Energy Procedia* 52 (2014) 438-448.
- [3] Ky, Thierry. S. M., Kam, Sié., Dianda, Boureima and Bathiebo, D. Joseph. Optical analysis of a hemispheric concentrator with a manual tracking system for the declination. *Global Journal of Pure and Applied Sciences*. Vol 21, 2015: 145-154.
- [4] M. F. El-Refai. Performance analysis of the stationary-reflector/tracking absorber solar collector. *Applied Energy*, 28 :163–189, 1987.

- [5] K. M. Ng, N. M. Adam, and B. Z. Azmi. Numerical simulation on the reflection characterization and performance of a solar collector - a case study of upm solar bowl. *Science and Technology*, 20 :283–298, 2012.
- [6] Nadia Bouguetaia. Contribution à l'étude et à la simulation d'un concentrateur cylindro-parabolique. Master's thesis, Université Constantine 1 Faculté Des Sciences Exactes, 2013.
- [7] Steward W. G. and Kreith F., Stationary concentrating reflector cum tracking absorber solar energy collector: optical design characteristics. *Applied optics*. Vol 14, No.7, 1975.
- [8] Williams B. Stine, Michael Geyer, and R. W. Harrigan. *Solar energy systems design*. Solar Power System, 1986.
- [9] François Veynandt. Congénération hélio thermodynamique avec concentrateur linéaire de fresnel : modélisation de l'ensemble du procédé. PhD thesis, Institut National Polytechnique de Toulouse (INP Toulouse), 2011.
- [10] R. Bernard, G. Menguy, M. Schwartz. *Le rayonnement solaire, Conversion thermique et applications*. Editions Tec-Doc, 1980.
- [11] M. Yusof Sulaiman, W. M. Hlaing Oo, Mahdi AbdWahab, Z. Abidin Sulaiman and K. Y. Khouzam. Conceptual design of a hybrid thermal and photovoltaic receiver of a FMDF collector. *Renewable Energy*, Vol. 12, No. 1, pp. 91-98, 1997.